10

Photocatalytic and Adsorption Properties of $ZnO/ZnAl_2O_4/Cu$ Nanocomposites

© A. Tincu[1], A.A. Shelemanov[1], S.K. Evstropiev[1,2,3]

[1] ITMO University, St. Petersburg, Russia
[2] St. Petersburg State Technological Institute (Technical University), St. Petersburg, Russia
[3] NPO„Vavilov State Optical Institute“,
192171 St. Petersburg, Russia

e-mail:

Received September 28, 2022
Revised November 25, 2022
Accepted December 04, 2022

Experimental results on photobleaching of Chicago Sky Blue diazo dye solutions using $ZnO/ZnAl_2O_4/Cu$ photocatalytic nanocomposites are presented. Data on the crystal structure and morphology of these nanocomposites obtained by the polymer-salt method are presented. The results of studies of the kinetics of the processes of photobleaching of dye solutions and its adsorption on the surface of powdered nanocomposites showed that the experimental data correspond to known kinetic models using the first and second order rate equations for these processes.

Keywords: dye, photobleaching, solution, photocatalysis, adsorption.

DOI: 10.61011/EOS.2023.03.56190.4154-22

Introduction

Many countries are currently developing semiconductor oxide photocatalytic materials for power generation and advanced air and water purification systems [1–7].

It is known (e.g., [1–3] that the photocatalysis process involves light absorption by a semiconductor material, generation of electron-hole pairs, their transport to the material surface and formation there of chemically active particles (hydroxide – radical ·OH, anions $\cdot O_2^-$ and others) that degrade organic contaminants [1–3]. Therefore, the role of processes occurring during photocatalysis on the surface of materials is very important. The increase in specific surface area achievable with nanoscale materials is used to increase the efficiency of photocatalytic processes.

Mechanical dispersion methods can be used to increase the specific surface area of the materials, but it is more efficient to use special methods to produce nanoscale photocatalysts, such as – gel synthesis [1], solution combustion method [3], polymer – salt method [4], solution deposition 5,8 and others.

In photocatalytic decomposition, the interaction of organic molecules with the photocatalyst takes place on its surface. This determines the importance of taking into account the adsorption of organic molecules on the photocatalyst surface. The adsorption processes of organic pollutants on the surface of photocatalysts have been investigated previously in papers [9–15].

One of the most effective photocatalysts is zinc oxide-based materials [1–5, 16–18]. To enhance the photocatalytic properties of zinc oxide various additives are widely used that change the morphology of the material, increase its specific surface area, reduce the probability of recombination processes of electronically generated – hole pairs (e.g., [4,19,20]). The application of $ZnAl_2O_4$ as photocatalytic material was investigated in [21–23]. The high photocatalytic properties of ZnO-Cu nanocomposites have been reported in a number of papers [24–26]. The photocatalytic properties of $ZnAl_2O_4$ have been shown is [8] to increase when copper is added to the material composition.

The aim of this paper was to investigate the photocatalytic and adsorption properties of $ZnO/ZnAl_2O_4/Cu$ nanocomposites produced by the polymer – salt method.

Materials and methods

The polymer – salt method described in detail earlier in [4,20] was used to synthesize the nanocomposites. Aqueous solutions of $Zn(NO_3)_2$, $Al(NO_3)_3$, $CuSO_4$ and a solution of Polyvinylpyrrolidone (PVP) in Propanol-2 were used as starting materials. The solutions were mixed in the specified volumes using a magnetic stirrer. The resulting homogeneous composite solutions were placed in a Fisher Scientific drying cabinet. Drying was carried out for 96 h at temperature 75°C.

The heat treatment of the dried samples was carried out in a Nabertherm N20/HR electric laboratory furnace at 680°C for 2 h with an exit time of 2 h. The heat treatment mode used ensured complete decomposition of PVP and metal nitrates with the formation of oxide nanocomposites.

The chemical compositions of the solutions and the oxide composites obtained from them are given in the Table.

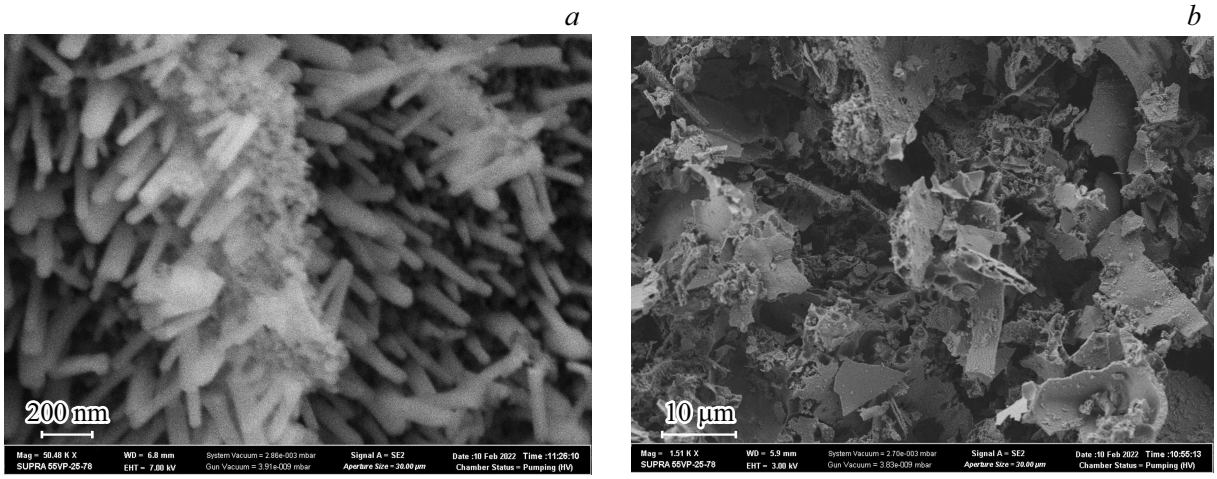

Figure 1. Electron microscopic images (with different magnifications) of nanocomposite **1**.

Table 1. Chemical composition of the solutions and the composites obtained therefrom

Number	Chemical composition of solutions, mass %						Chemical composition of composites, mol %		
	H_2O	PVP	Propanol-2	$Zn(NO_3)_2 \cdot 6H_2O$	$Al(NO_3)_3 \cdot 6H_2O$	$CuSO_4 \cdot 5H_2O$	ZnO	$ZnAl_2O_4$	CuO*
1 Zn_4-Cu03	51.6	2.58	40.60	3.38	1.77	0.013	82.91	16.69	0.40
2 Zn_1-Cu03	53.0	2.65	41.7	1.76	3.54	0.011	–	99.6	0.40

Scanning electron microscopy was used to investigate the morphology of the obtained materials. A Supra 55VP electron microscope was used for the research.

The crystalline structure of the synthesized powders was studied by X-ray diffraction analysis on a Rigaku Ultima IV apparatus. The Scherrer formula was used to estimate the crystal size from the data obtained.

Chicago Sky Blue (CSB) diazo dye (Sigma Aldrich) was used as a model organic pollutant. The powder weights used in the experiments were 0.01 g. Powder suspensions were mixed with 3 ml aqueous dye solution (all dye solutions are further aqueous) and placed in a quartz cuvette. The content of the dye in the initial solutions was 42 mg/l. This dye was used earlier in [3,5,9,17,18] to evaluate the photocatalytic properties of materials.

In dye solutions, an intense absorption band with a maximum of $\lambda_{max} = 612$ nm is observed. In [9] the experimentally determined dependence of the absorbance of CSB solutions at this wavelength on the dye concentration was given. In the present study, this dependence was used to determine the concentration of the dye in the studied solutions.

A high-pressure mercury lamp DRSH-250 was used to phototreat solutions. The emission spectrum of this lamp has been given in [27].

The absorption spectra of the solutions were measured on a Perkin Elmer Lambda 900 spectrophotometer in the 300–750 nm spectral range using standard 10 mm quartz cuvettes.

Fig. 1 shows electron microscopic images (with different magnifications) of the **1** nanocomposite. It can be seen from Fig.1, *a* that the synthesized powder is composed of microscopic particles of different sizes and shapes. A higher magnification image showed that these particles contain pores and are composed of smaller particles of no more than 50 nm. This morphology of the material can provide a large surface area of contact between the material and the environment, which contributes to its adsorptive and photocatalytic properties.

A study of the structure of $ZnO/ZnAl_2O_4/Cu$ nanocomposites by X-ray diffraction analysis in the early papers [28] showed that the obtained materials consist of a mixture of small and tightly packed hexagonal ZnO crystals (size 8–13 nm) and cubic spinel crystals $ZnAl_2O_4$. It was found that copper ions were incorporated into the crystalline lattice of zinc oxide, slightly changing the parameters of its lattice cell.

Photobleaching of dye solutions

Fig. 2 shows the change in absorption spectra of a CSB dye solution containing **2** powder additives under UV irradiation. The figure shows that the irradiation causes gradual solution bleaching, while the form of the dye

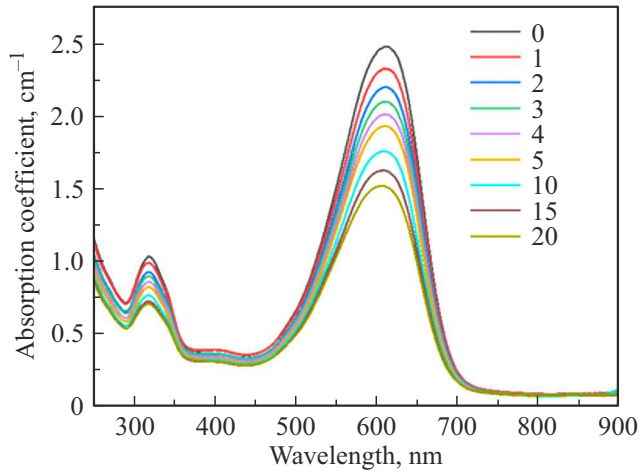

Figure 2. Absorption spectra of Chicago Sky Blue dye solutions containing powder **2**, before exposure (0) and after UV irradiation for 1,2,. . . 20 min.

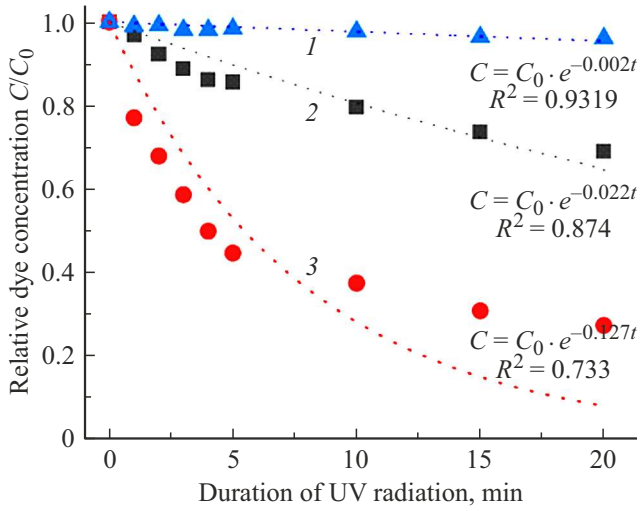

Figure 3. Photobleaching curves of CSB dye solution (curve *1*) and solutions of this dye containing photocatalytic powder additives **2** (curve *2*) and **1** (curve *3*).

absorption spectrum remains unchanged. This suggests that the resulting photodegradation products have no significant effect on the absorption spectra of the dye in the visible part of the spectrum. The observed pattern of change in the dye absorption spectra is broadly similar to that previously described in [12].

Fig. 3 shows the bleaching kinetic curves of CSB solution (curve *1*) as well as solutions of this dye containing powder additives **1** (curve *3*) and **2** (curve *2*). For samples **1** and **2** the graphs are shown with adsorption taken into account. The photobleaching process of CSB solution without addition of powders is relatively slow — at a UV irradiation time of 25 min less than 5% of the dye molecules are observed to decompose. The figure shows that the photobleaching rate of the solution increases considerably with the addition of synthesized powders, with a significantly higher acceleration of the decolorization being observed with the addition of **1** powder containing zinc oxide.

The light absorption by dye molecules in solution is a photochemical decomposition reaction. The speed of this process is described by a first-order reaction kinetic model:

$$C = C_0 e^{-k_{app}t}, \qquad (1)$$

where C_0 — initial dye concentration in solution (mg/l), C — current dye concentration (mg/l);k_{app} — nominal pseudo-first order reaction rate constant (min^{-1}). To formally describe the photobleaching kinetics of solutions containing organic dyes and photocatalytic additives, the first-order reaction kinetic equation [4,5,9,12,13,17] is also often used.

The curves based on calculations using the formula (1) and experimental data are shown in Fig. 3. These curves do not describe the experimental data well enough. The value of the coefficient of determination R to estimate the fit of the kinetic model to the experimental values does not exceed 0.9 for samples **1** and **2**, which indicates the inapplicability of this kinetic model. This may be due to the high adsorption properties of the nanocomposites **1** and **2**.

For a more accurate description of the photobleaching kinetics, a pseudo-second-order reaction photocatalysis kinetic model was chosen, which can be written in [13] form:

$$\frac{1}{c} = \frac{1}{c_0} + K_2 t, \qquad (2)$$

where k_2 – the rate constant of a pseudo-second order photocatalytic reaction. Fig. 4 shows the $1/C = f(t)$ dependence plots for dye photodegradation when using **1** and **2** nanocomposites. It can be seen that the experimental data for dye photodecomposition using both composites are well described by the pseudo-second order kinetic dependence ($R^2 > 0.9$).

It is known that the photobleaching of solutions in the presence of dispersed photocatalysts is determined by several processes [9–15,29]:

- photodegradation of dye molecules in the solution;
- by dye adsorption on the surface of a dispersed photocatalyst;
- by photocatalytic decomposition of dye molecules on the photocatalyst surface.

The rate of each of these processes and their contribution to the photobleaching of solutions depends on a number of factors, including chemical composition, photocatalyst structure and morphology, dye concentration in the solution, spectral composition and intensity of radiation used, temperature and other conditions of photochemical treatment. In the irradiation process, dye removal from the solution is determined both by its decomposition (in the liquid phase or on the photocatalyst surface) and by its adsorption on the dispersed photocatalytic powder surface). These phenomena have been discussed in some detail in [9,11–15,17,29].

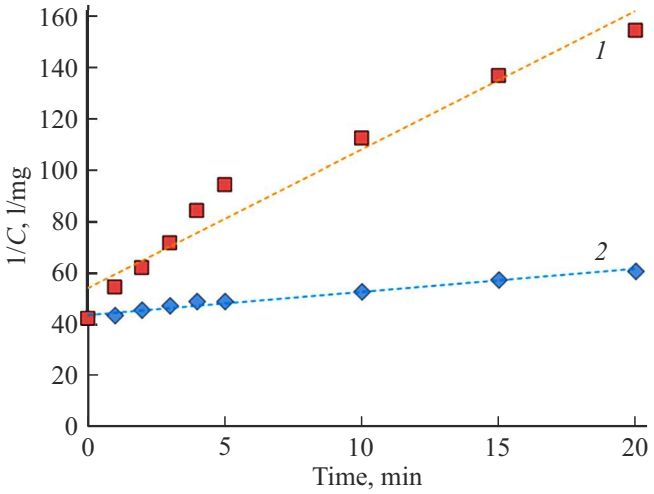

Figure 4. Dependences $1/C = f(t)$ for dye photodecomposition processes by applying nanocomposites **1** and **2** and their linear approximation results by functions $5.4025t + 54.31$ and $0.8954t + 43.69$.

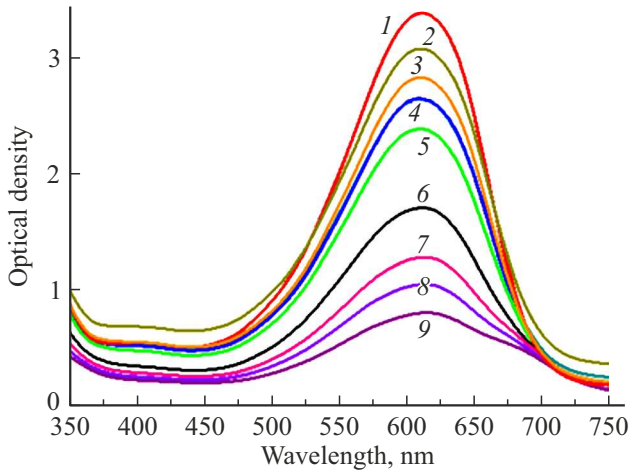

Figure 5. Changes in the absorption spectrum of Chicago Sky Blue dye solution during adsorption on the surface of the powder **1**. Adsorption process duration, min: 0 (original solution, curve *1*), 5 (curve *2*), 10 (curve *3*), 15 (curve *4*), 20 (curve *5*), 30 (curve *6*), 40 (curve *7*), 50 (curve *8*), 60 (curve *9*).

Kinetics of Chicago Sky Blue dye adsorption from solutions

To evaluate the effect of adsorption on the photobleaching kinetics of the dye solution, experiments were carried out in the absence of external radiation at 1 h process duration corresponding to the experimental data on photobleaching of solutions (Fig. 3, 4). Fig. 5 shows the effect of dark exposure of CSB solution containing **1** powder on the absorption spectra of the solution. It can be seen that the nature of the spectral changes is similar to that observed in photobleaching of the solution (Fig. 2). This Fig. shows the experimental results showing the changes during the initial stage of the adsorption process and corresponds to the photobleaching of the solution (curve 3, Fig. 3).

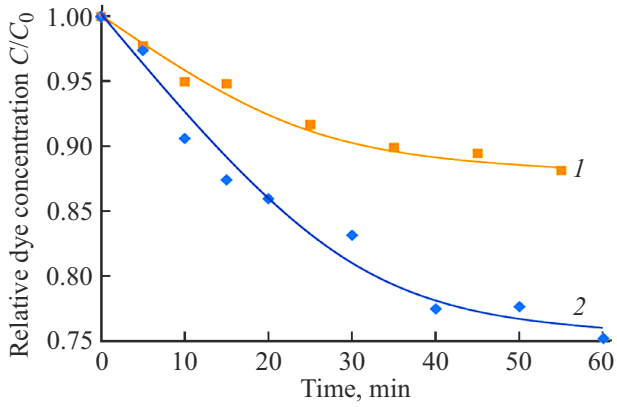

Figure 6. Kinetic dependences of dye adsorption in darkness conditions on the surface of **2** (curve *1*) and 1 (curve *2*) powders.

Fig. 6 shows the kinetic dependence of dye adsorption under darkness conditions on the surface of **1** and **2** powders. Comparison of the results with photobleaching of solutions (Fig.3) shows that the dye adsorption on the surface of the materials are significantly slower than the observed bleaching of solutions under UV irradiation. Similar results were obtained earlier in paper [9].

When considering photocatalytic processes, kinetic models of adsorption on the surface of solids, including pseudo-first and pseudo-second order equations, are most commonly used [5,9,12].

In the pseudo-first order kinetic equation [9,12,18,19,30] the adsorption rate is described by the expression [12,30]:

$$\frac{dq_t}{dt} = k_1(q_e - q_t), \tag{3}$$

where q_t (mmol/g) — the amount of dye adsorbed to 1 g sorbent by time t;q_e(mmol/g) — the equilibrium adsorption capacity of the sorbent;k_1 (min^{-1}) — adsorption rate constant; t — duration of adsorption process (min). According to equation (3), the speed of the adsorption process decreases as the surface is filled with dye molecules. In the present paper, q_e values were calculated based on dye concentration in solutions at the duration of adsorption process ~60 min and are close to the equilibrium adsorption capacity of the outer surface of photocatalyst particles.

Fig. 7 shows the $ln(q_e - q_t) = f(t)$ dependencies based on experimental data for **1** (Fig.7, *a*) and **2** (Fig.7, *b*) dye adsorption. The above data show that the linear dependences given correspond satisfactorily ($R^2 > 0.9$) to the experimental results for adsorption on the surface of both powders. Comparing the values of k_1=0.0073 (*a*) and 0.0026 min^{-1} (*b*) shows that the process proceeds much faster on the surface of **1** powder containing more zinc oxide. This can be explained by the manifestation of the interaction between CSB molecules and Zn^{2+} ions described earlier in [9].

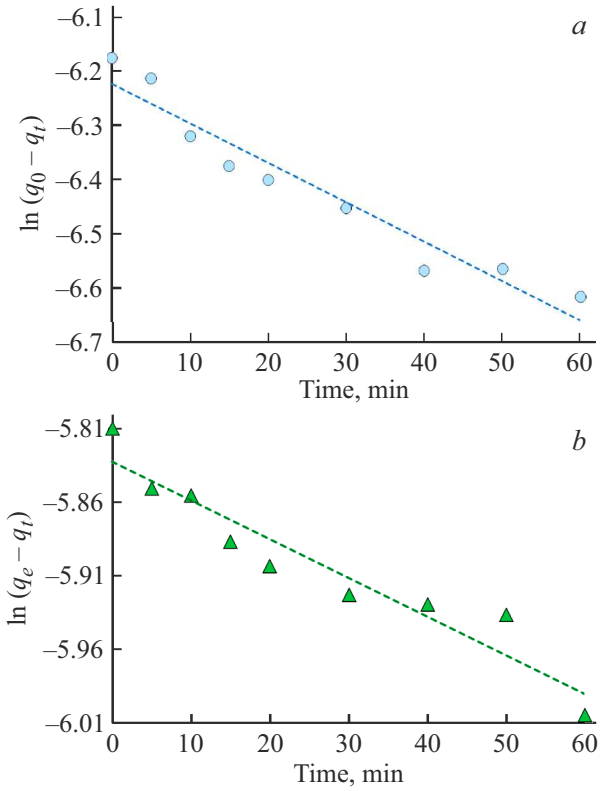

Figure 7. Dependencies $\ln(q_e - q_t) = f(t)$ plotted from experimental data on dye adsorption of powders **1** (*a*) and **2** (*b*).

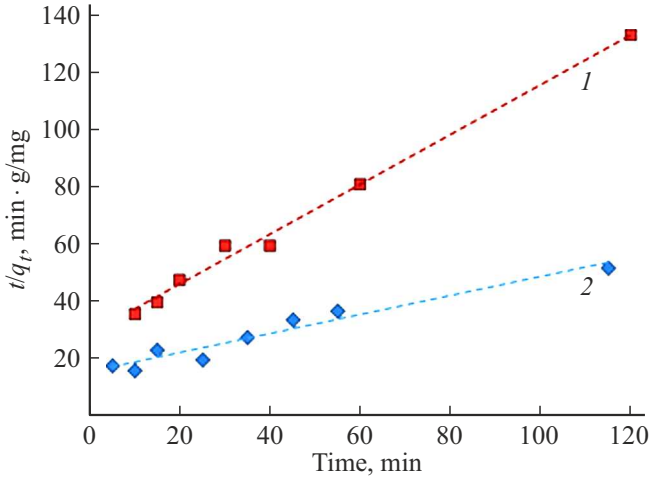

Figure 8. Time dependences of t/q_t plotted on Chicago Sky Blue (Sigma Aldrich) dye adsorption from aqueous solution on powder surfaces **1** (*1*) and **2** (*2*), and their linear approximation to $0.870t + 28.29$ and $0.329t + 15.64$.

It can also be noted that the rate constant of adsorption of CSB dye on the surface of ZnO-MgO nanocomposite ($k_1 = 0.056$) given in [12] in the present paper is significantly higher than that obtained in the present paper. This can be explained by significant differences both in chemical composition and structure of nanocomposites obtained in the present paper and in [12], significant difference in conditions of adsorption kinetics experiments (different concentrations of initial solutions and masses of composite suspensions).

To describe the kinetics of adsorption from solutions, a pseudo-second-order equation is often used, which can be written in the

$$\frac{dq_t}{dt} = k_2(q_e - q_t)^2, \tag{4}$$

form or in the integrated form [12,26,30–32]:

$$\frac{t}{q_t} = \frac{1}{k_2 \times q_e^2} + \frac{t}{q_e}, \tag{5}$$

where k_2 – second order adsorption rate constant, q_e – maximum equilibrium adsorption capacity of the powder (mg/g), q_t – adsorbed dye content on the surface of the powder at duration of adsorption process t.

The graph $\frac{t}{q_t} = f(t)$ (Fig. 8) showed a good agreement ($R^2 = 0.992$) of the experimental data with Equation (5). Thus, the kinetics of CSB dye adsorption from solutions onto the surface of obtained powders in the considered main stage of solution decolorization (removal of up 80% dye molecules from solutions) is satisfactorily described by kinetic models of both first and second orders.

Thus, the experimental results on photobleaching kinetics of CSB diazodye solutions and adsorption of this dye on ZnO/$ZnAl_2O_4$/CuO photoactive powder surfaces show that the rates of these processes are satisfactory described by the known kinetic models. The photobleaching processes of solutions are satisfactorily described by the pseudo-second-order kinetic dependence, which agrees well with the literature data on photocatalysis in the application of some other oxide photocatalysts[4,9,12].

Conclusions

ZnO/$ZnAl_2O_4$/Cu nanocomposites synthesized by polymer-salt method showed high photocatalytic and adsorption properties in decolorizing aqueous solutions of Chicago Sky Blue dye. Experimental data showed that the rate of dye adsorption and photobleaching of solutions under UV radiation was higher when using nanocomposites with a higher zinc oxide content. It was found that the photo-bleaching rate of diazo dye solutions in ZnO/$ZnAl_2O_4$/Cu nanocomposites significantly exceeds the adsorption rate on the nanocomposite particles in the absence of UV irradiation. A study of the adsorption kinetics of dye nanocomposites from these solutions showed that the kinetic model describing the adsorption rate by a pseudo-second order equation better fits the experimental data obtained than the model describing the adsorption kinetics by a pseudo-first order equation.

References

[1] X. Chen, Z. Wu, D. Liu, Z. Gao. Nanoscale Research Lett.,**12**, 143(2017). DOI: 10.1186/s11671-017-1904-4

[2] R. Kumar, G. Kumar, A. Umar. Mater. Lett., **94** (15), 100(2013). DOI: 10.1016/j.matlet.2013.01.044

[3] N. Srinatha, V. Kumar, K. Nair, B. Angadi. Adv. Powder Technol., **26** (5), 1355(2015). DOI: 10.1016/J.APT.2015.07.010

[4] S.K. Evstropiev, L.V. Lesnykh, A.V. Karavaeva, N.V. Nikonorov, K.V. Oreshkina, L.Yu. Mironov, S.Yu. Maslennikov, E.V. Kolobkova, I.V. Bagrov. Chem. Engineering and Processing−Process Intensification, **142**, 107587(2019). DOI: 10.1016/j.cep.2019.107587

[5] L.M. Jose, R.S. Arun Raj, D. Sajan, A. Aravind. Nano Express, **2** (1), 010039(2021). DOI: 10.1088/2632-959X/abeec6

[6] A. Mills, S. Le Hunte. J. Photochem. Photobiol. A: Chem., **108** (1), 1(1997). DOI: 10.1016/S1010-6030(97)00118-4

[7] S. Ahmed, C.E. Jones, T.J. Kemp, P.R. Unwin. Phys. Chem. Chem. Phys., **1** (1999) 5229-5233. DOI: 10.1039/A906819H

[8] F.Z. Akika, M. Benamira, H. Lahmar, M. Trari, I. Avramova, S. Suzer. Surface and Interfaces, **18**, 100406(2020). DOI: 10.1016/j.surfin.2019.100406

[9] A.S. Saratovskii, D.V. Bulyga, S.K. Evstropiev, T.V. Antropova. Glass Physics and Chemistry, **48** (1), 10(2022). DOI: 10.1134/S1087659622010126.

[10] L. Zhang, M. Jaroniec. In: *Surface Science of Photocatalysis*, ed. by J. Yu, M. Jaroniec, C. Jiang. Interface Science and Technology (Elsevier, 2020), v. 31, p. 39–69.

[11] A. Gara, V.K. Sangal, P.K. Bajoai. Desalination and Water treatment, **57** (38), 18003(2016). DOI: 10.1080/19443994.2015.1086697

[12] D.V. Bulyga, S.K. Evstropiev, Opt. and Spectr., **130** (9), 1455(2022). (in Russian). DOI: 10.21883/OS.2022.09.53309.3617-22

[13] M. Irani, T. Mohammadi, S. Mohebbi. J. Mex. Chem. Soc., **60** (4), 218(2016). DOI: 10.29356/jmcs.v60i4.115

[14] S. Natarajan, H.C. Bajaj, R.J. Tayad. J. Environmental Sci., **65**, 201(2018). DOI: 10.1016/j.jes.2017.03.011

[15] J. Chen, Y. Xiong, M. Duan, X. Li, J. Li, S. Fang, S. Qin, R. Zhang. Langmuir, **36** (2) 520(2019). DOI: 10.1021/acs.langmuir.9b02879

[16] U.I. Gaya, A.H. Abdullah. J. Photochem. Photobiol. C: Photochem. Rev., **9**, 1(2008). DOI: 10.1016/j.jphotochemrev.2007.12.003

[17] H.Y. Zhu, R. Jiang, Y.-Q. Fu, R.-R. Li, J. Yao, S.-T. Jiang. Appl. Surf. Sci., **369**, 1(2016). DOI: 10.1016/j.apsusc.2016.02.025

[18] S. Lagergren. Kung Sven Veten Hand, **24** (1), 39(1898).

[19] T.T. Minh, N.T.T. Tu, T.T.V. Thi, L.T. Hoa, H.T. Long, N.H. Phong, T.L.M. Pham, D.Q. Khieu. J. Nanomater., **2019**, 5198045(2019). DOI: 10.1155/2019/5198045

[20] A.A. Shelemanov, S.K. Evstropiev, A.V. Karavaeva, N.V. Nikonorov, V.N. Vasilyev, Y.F. Podruhin, V.M. Kiselev. Mater. Chem. Phys., **276**, 125204(2022). DOI: 10.1016/j.matchemphys.2021.125204

[21] E.L. Foletto, S. Battiston, J.M. Simões, M.M. Bassaco, L.S.F. Pereira, É.M.M. Flores, E.I. Müller. Microporous and Mesoporous Materials, **163**, 29(2012). DOI: 10.1016/j.micromeso.2012.06.039

[22] C.G. Anchieta, D. Sallet, E.L. Foletto, S.S. da Silva, O. Chiavone-Filho, C.A.O. do Nascimento. Ceram. Int., **40** (3), 4173(2014). DOI: 10.1016/j.ceramint.2013.08.074

[23] A. Chaudhary, A. Mohammad, S.M. Mobin. Materials Science and Engineering B, **227**, 136(2018). DOI: 10.1016/j.mseb.2017.10.009

[24] A. Khalid, P. Ahmad, A. Khan, S. Muhammad, M.U. Khandaker, Md.M. Alam, M. Asin, I.U. Din, R.G. Chaudhary, D. Kumar, R. Sharma, M.R.I. Faruque, T.B. Emran. Chem. Appl., **2022**, 9459886(2022). DOI: 10.1155/2022/9459886

[25] H.R. Mardani, M. Forouzani, M. Ziari, P. Biparva. Spectrochimica Acta Part A: Molecular and Biomolecular Spectroscopy, **141**, 27(2015). DOI: 10.1016/j.saa.2015.01.034

[26] M. Shirzad-Siboni, A. Jonidi-Jafari, M. Farzadkia, A. Esrafili, M. Gholami, J. Environmental Management, **186**, 2917(2016). DOI: 10.1016/j.jenvman.2016.10.049

[27] S.K. Evstropiev, V.N. Vasilyev, N.V. Nikonorov, E.V. Kolobkova, N.A. Volkova, I.A. Boltenkov. Chemical Engineering and Processing: Process Intensification, **134**, 45(2018). DOI: 10.1016/j.cep.2018.10.020

[28] A. Tinku, A.A. Shelemanov, S.K. Evstropiev. Opt. i spektr., **130** (10), 1571 (2022). (in Russian). DOI: 10.21883/OS.2022.10.53628.3275-22

[29] W. Zou, B. Gao, Y.S. Ok, L. Dong. Chemosphere, **218**, 845(2019). DOI: 10.1016/j.chemosphere.2018.11.175

[30] Y. Kuang, X. Zhang, S. Zhou. Water, **12**, 587(2020). DOI: 10.3390/w12020587

[31] Y.-S. Ho. J. Hazard. Mater., **136** (3) 681(2006). DOI: 10.1016/j.jhazmat.2005.12.043

[32] J.C. Bullen, S. Sleesongsom, K. Gallagher, D.J. Weiss. Langmuir, **37** (10), 3189(2021). DOI: 10.1021/acs.langmuir.1c0014

Translated by Y.Deineka